Opportunistic high cross-range resolution imaging using TOPSAR illuminations of Sentinel-1

Virginie Kubica[(1,2)], Xavier Neyt[(1)] and Hugh Griffiths[(2)]
[(1)] Dept. of Electrical Engineering, Royal Military Academy, Belgium
{Virginie.Kubica, Xavier.Neyt}@rma.ac.be
[(2)] Dept. of Electronic and Electrical Engineering, University College London, UK
Hugh.Griffiths@ucl.ac.uk

Abstract *Burst mode SAR's such as ScanSAR or TOPSAR can achieve wide swath coverage in a single pass of the satellite at the cost of degraded cross-range resolution. In the bistatic configuration using a SAR satellite as illuminator of opportunity and a ground-based stationary receiver close to the imaged area, this coarse cross-range resolution can be improved in some favourable geometries by exploiting the sidelobe emissions of the beams illuminating the adjacent sub-swaths. This paper compares the oustanding performance that can be achieved in ScanSAR and TOPSAR mode thanks to a bistatic geometry.*

Introduction

Compared to the narrow-swath high-resolution Stripmap SAR imaging mode, wide-swath SAR imaging modes offer a short-revisit interval and a global coverage by sweeping the antenna beam sequentially from near range to far range. One of the most important wide-swath modes is the ScanSAR mode [1] which was first implemented on RADARSAT-1 and later on ENVISAT and RADARSAT-2. To alleviate the drawbacks of the ScanSAR mode, such as the well-known scalloping effect, another wide-swath mode, called TOPS (Terrain Observation by Progressive Scan) imaging mode, has been first discussed in [2] and is now the main mode of operation for the recently launched ESA's satellite Sentinel-1. While in the ScanSAR mode the antenna is steered only in the range direction, in TOPSAR mode, the antenna is steered in both azimuth and range. In those wide-swath modes, the synthetic aperture length is shared between beam positions, so the cross-range resolution is poorer. Table 1 draws up a non-exhaustive list of wide-swath modes implemented on SAR satellites and their spatial resolution with δ_r and δ_{az} respectively the range and the cross-range resolution. One can see that the TOPSAR imaging mode implemented on Sentinel-1 [3] is characterized by an imbalance between the range and the cross-range resolution which means that improving this coarse cross-range resolution in bistatic operation is more valuable in TOPSAR mode compared to ScanSAR mode.

Table 1: A non-exhaustive list of wide-swath imaging satellites and their monostatic spatial resolution.

SAR satellites	Mode	δ_r x δ_{az} (m)
ASAR ENVISAT	ScanSAR WS	150 x 150
	ScanSAR GM	1000 x 1000
RADARSAT-2	ScanSAR narrow	37.7-79.9 x 60
	ScanSAR wide	72.1-160 x 100
Sentinel-1	TOPSAR IW	2.7-3.5 x 22
	TOPSAR EW	7.9-15 x 43

In [4, 5], it was demonstrated that the coarse monostatic cross-range resolution of ScanSAR mode can be enhanced in the case of a bistatic configuration with a receiver close to the imaged area by exploiting the sidelobe emissions of the beams illuminating the adjacent sub-swaths. This cross-range resolution enhancement method can restore the cross-range resolution of the Stripmap mode provided that the amplitude of the signals transmitted in the sidelobes of the ScanSAR beams is sufficient. This is the case in geometries for which the sidelobe radiations of the ScanSAR beams which illuminate the adjacent sub-swaths also illuminate the sub-swath in which the receiver and the imaged area are located. In this paper, the performance of the innovative method are assessed in the case of TOPSAR illuminations.

Passive SAR system

The passive SAR system considered in this paper is shown in Fig. 1 and consists in an opportunistic spaceborne transmitter operating in wide-swath mode and a stationary ground-based receiver.

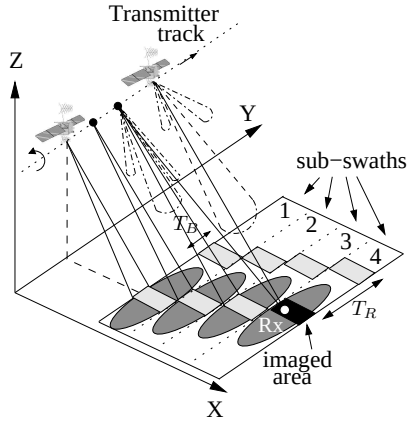

Figure 1: Bistatic acquisition geometry in wide-swath imaging mode in the case of four sub-swaths. The receiver and the imaged area are located at the edge of the global swath (dark area) and are illuminated by the sidelobes of the beam illuminating sub-swath 3 and afterwards, by the mainlobe of the beam illuminating sub-swath 4.

The receiving system, represented on Fig. 2 is a heterodyne receiver tailored for the C-band (ENVISAT, RADARSAT-1/2, Sentinel-1). The scattered signals are received via a wide-

beam patch antenna and routed through a band-pass filter, a cascade of LNAs (Low Noise Amplifier) and an analog down-converter. They are then sampled at 50 MSamples/s using a 16-bit A/D card (AlazarTech ATS660) after an anti-aliasing filter before being digitally down-converted to base-band and stored for offline processing and analysis. Next, signal separation is performed to extract the reference signal (direct-path signal) from the reflected signal. In the present case, the reference signal is re-synthesized since its general shape is known. Finally, an image is synthesized from the separated signals using a bistatic back-projection algorithm [6].

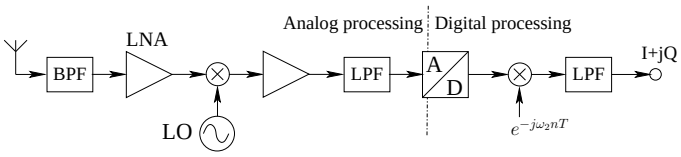

Figure 2: Signal Processing diagram of one receiver chain with an analogue (ADC) followed by a digital down-conversion (DDC).

Burst-mode illumination in bistatic operation

The principle of ScanSAR is sketched in Fig. 1, where the geometry of a four sub-swaths ScanSAR is shown. Each sub-swath is illuminated by the antenna beam for a short time interval, T_B and it will return to the same sub-swath after time T_R, called cycle time. In TOPSAR mode, in addition to the range scanning, the antenna beam is steered during the acquisition of each burst from back to fore, i.e. in the opposite direction of spotlight mode. This results in a virtual shrinking of the AAP. In monostatic ScanSAR imaging, the dwell-time T_D, i.e. the azimuth integration time for a point target, is identical to the burst duration T_B, which is not the case in TOPSAR mode where the burst duration is longer to ensure a sufficient dwell-time on target.

The bistatic geometry considered in this work allows the receiving system to receive echoes issued from the sidelobes emissions of the adjacent beams from the transmitter. This is possible thanks to the short reflected path from the observed area and also because of the attenuation by the one-way transmit antenna gain pattern and not by the two-way antenna pattern. Figure 3 (a) depicts the acquired signal during an overpass of Sentinel-1 operating in the Interferometric Wide-swath mode (IW) over the ground-based receiving system in Brussels. The dashed lines demarcate each T_B, i.e. the time interval spent by the beam on each sub-swath. In this TOPSAR mode, the monostatic dwell-time would be of 0.24 sec (duration of the mainlobe of the shrunk AAP) while in this bistatic configuration, the dwell-time on target is of 2 sec, which is the entire length of this acquisition. Figure 3 (b) represents the received signal from RADARSAT-2 operating in ScanSAR Wide mode B (SWB) characterized by 4 beams or sub-waths. The dashed lines demarcate each T_R, i.e. each group of 4 beams. In this case, the monostatic dwell-time would be of 0.05 sec (duration of one burst) while in this bistatic configuration, the dwell-time on target is of 0.6 sec, again the entire length of this acquisition. This bistatic long dwell-time on target is possible if the receiver and the surrounding observed area are located in the center of the global swath. This longer dwell-time will result in a higher integration gain.

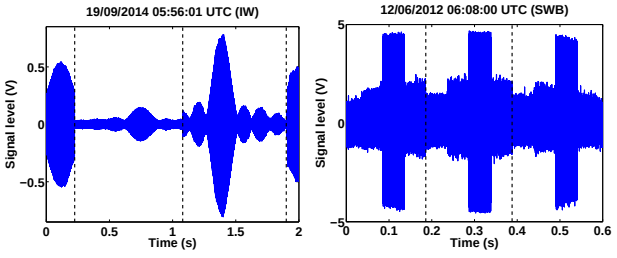

Figure 3: Acquired signals in wide-swath mode: (a) TOPSAR illumination of Sentinel-1 operating in IW mode and (b) 3 cycles of a ScanSAR illumination of RADARSAT-2 operating in SWB.

Cross-range resolution enhancement method

Let first define the signal model on which the cross-range resolution enhancement method is based. The imaged area consists of K ground patches. All measurement samples in time and space are stacked into a single measurement vector $\mathbf{y} \in \mathbb{C}^{\mathbf{MN\times 1}}$ with M the number of transmitted pulses and N the number of range cells. The total received signal is the sum of the responses from all ground patches and can be modeled as

$$\mathbf{y} = \mathbf{H_w x} + \mathbf{n} \tag{1}$$

where the k^{th} column of $\mathbf{H_w} \in \mathbb{C}^{\mathbf{MN\times K}}$ represents a received signal if a scatterer at ground patch k has a reflection coefficient of 1. The subscript in $\mathbf{H_w}$ refers to the azimuth modulation experienced by the imaged ground patch. The elements of the column vector $\mathbf{x} = [x^0, x^1, ..., x^k, ..., x^{K-1}]^T$ are the complex reflectivity of each ground patch and $\mathbf{n} \in \mathbb{C}^{\mathbf{MN\times 1}}$ denotes the thermal noise, assumed complex Gaussian. In the bistatic geometry considered in this work, each ground patch in the observed scene is assumed to experience the same AAP as the receiver since the imaged area is close to the receiver and small. Therefore, $\mathbf{H_w}$ can be rewritten as

$$\mathbf{H_w} = \mathbf{W} \odot \mathbf{H} \tag{2}$$

where $\odot$ denotes the Hadamard multiplication and the matrix $\mathbf{H}$ has a unity constant amplitude. The column of the matrix $\mathbf{W}$ are identical and equal to $\mathbf{w}$, the slow-time amplitude modulation which corresponds to the envelope of the signals shown on Fig. 3.

The SAR focusing using the cross-range resolution enhancement method developed in [4, 5] can be written as

$$\hat{\mathbf{x}} = \mathbf{H}^{\dagger}\mathbf{C_w y} \tag{3}$$

where the matrix $\mathbf{C_w}$ is a diagonal matrix with the diagonal elements equal to

$$c_{w,i} = \frac{w_i}{w_i^2 + \vartheta} \tag{4}$$

with $\vartheta = \frac{\sigma_n^2}{\sigma_x^2}$ the inverse of the SNR, σ_n^2 being the variance of the noise and σ_x^2 the variance of the reflectivity. The matrix $\mathbf{C_w}$ acts as a compensation of the azimuth modulation embodied by $\mathbf{w}$. Therefore, this method consists in

- compensating the AAP modulation of the measurements (rightmost product)

$$\mathbf{y_c} = \mathbf{C_w y} \tag{5}$$

- focusing using the conventional MF (leftmost product)

$$\hat{\mathbf{x}} = \mathbf{H}^{\dagger}\mathbf{y_c} \tag{6}$$

Note that the compensation (4) is optimum if the SNR embodied by ϑ is the true one. In reality, the SNR is not known and has to be estimated. The estimation of ϑ is very important as it defines how well the compensation of the azimuth modulation will happen. For an optimistic estimation of the SNR (ϑ too small), $\mathbf{c_w}$ tends to the inverse function of the azimuth modulation window $\mathbf{w}$, i.e. the signal as well as the underestimated noise will be compensated which results in an amplification of the noise. Whereas for a pessimistic estimation of the SNR (ϑ too large), neither the signal nor the noise are amplified. In other words, $\mathbf{c_w}$ strives to find a reasonable balance between, on the one hand, compensation of the weak signals and, on the other hand, amplification of the noise. In the sequel, the optimum value of ϑ is assumed known. It was demonstrated in [4, 5] that the noise amplification induced by the method does not strongly impact the SAR imaging if the illumination of the imaged area is continuous and if the pulses transmitted in the elevation sidelobes have sufficient SNR. Both conditions will be assessed in the case of TOPSAR imaging in the following section.

Performance in burst-mode illumination

In ScanSAR mode, the AAP is nearly constant within the burst duration which is not the case in TOPSAR for which the sidelobes of the shrunk sinc-shaped azimuth pattern also illuminate the scene as illustrated in Fig. 3 (a). As a result, the aforementioned condition of a continuous illumination can be more difficult to meet in TOPSAR mode since the amplitude of the transmitted signals in the sidelobes can be very small.
For illustrative purpose, a scenario with a point scatterer with a SNR before coherent processing, SNR_0, of -10 dB is simulated. The simulated azimuth modulation is based on the measured signal envelope of Fig. 3. The Integrated SideLobe Ratio (ISLR) and the Peak-to-SideLobe Ratio (PSLR) will be considered to assess the impact of respectively the TOPSAR and the ScanSAR mode on the image obtained. If the receiver/scatterer are located in the center of the global swath, reception of signals from all elevation beams is possible but each with a different amplitude according to the elevation antenna diagram of the considered beam as shown in Fig. 3. The spectrum of the respective azimuth modulation window predicts the azimuthal impulse response in the case of conventional Matched Filter (MF) processing. Figure 4 shows cuts of the Impulse Response Function (IRF) along the bistatic isorange. In ScanSAR illumination, the grating lobes resulting from the periodicity of the azimuth modulation window are reduced from PSLR = -8.8 dB (dashed line) to PSLR = -13.2 dB (solid line) using the cross-range-resolution method (5) as shown on Fig. 4 (b). The bistatic IRF in TOPSAR illumination is not characterized by grating lobes but by a high level of sidelobes. If the preprocessing step (5) is applied, the cross-range resolution is kept while the sidelobe levels considerably decrease as shown on Fig. 4 (a) from ISLR = 15 dB (dashed line) to ISLR = 11.2802 dB (solid line).

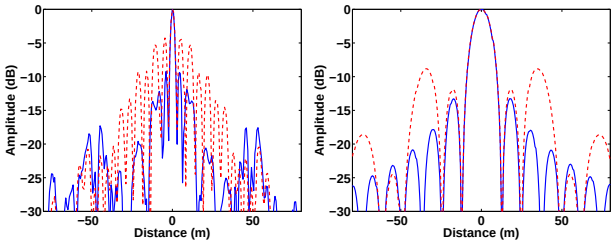

(a) (b)

Figure 4: IRF cuts along the scatterer's isorange using the conventional MF (dashed line) and the cross-range resolution-enhancement method (solid line) in (a) a TOPSAR illumination and (b) a ScanSAR illumination ($SNR_0 = -10$ dB) based on measurements of Fig. 3.

Conclusion

In this paper, we illustrate that, the coarse monostatic cross-range resolution of the TOPSAR mode can be improved by considering a bistatic configuration with a receiver close to the imaged area. This bistatic geometry offers a longer illumination of the scene by not only the elevation sidelobes of the shrunk AAP but also the beams illuminating the adjacent sub-swaths. Exploiting wide-swath modes illumination in the bistatic geometry studied in this work will significantly increase the frequency to have high cross-range SAR images. The cross-range resolution-enhancement method is even more valuable in TOPSAR mode compared to ScanSAR mode as the range resolution in TOPSAR is very good.
In the future, more TOPSAR measurements will help to confirm the results presented in this paper.

References

[1] R. Raney, A. Luscombe, E. Langham, and S. Ahmed, "RADARSAT," *Proceedings of the IEEE*, vol. 79, pp. 839–849, June 1991.

[2] F. De Zan and A. Monti Guarnieri, "TOPSAR: Terrain Observation by Progressive Scans," *IEEE Transactions on Geoscience and Remote Sensing*, vol. 44, no. 9, pp. 2352–2360, 2006.

[3] C. Thain, R. Barstow, and T. Wong, "Sentinel-1 Product Specification," tech. rep., MDA, 2011.

[4] V. Kubica and X. Neyt, "Feasibility of resolution-enhanced burst-mode interferometry in bistatic SAR," in *Proceedings of IEEE Conference on Radar*, (Adelaide, South Australia), Sept. 2013.

[5] V. Kubica and X. Neyt, "Cross-range resolution enhancement in burst-mode SAR in bistatic operation," in *Proceedings of the URSI 2012 Benelux Forum*, (Brusels, BE), p. 32, Sept. 2012.

[6] Y. Ding and D. Munson, "A fast back-projection algorithm for bistatic SAR imaging," in *Image Processing*, vol. 2, pp. 449–452, 2002.